Supplementary Information (SI) for Reaction Chemistry & Engineering.
This journal is © The Royal Society of Chemistry 2026

Supplementary Information (SI) for Reaction Chemistry and Engineering.

This journal is ©The Royal Society of Chemistry 2025

Zeolit-Catalyzed Solvent-Free Transoximation of Carbonyl Compounds and Cyclohexanone Oxime

Mengting Li [a], Yongrui Wang [a*], Yibin Luo[a*], Xingtian Shu[a]

a-Research Institute of Petroleum Processing, Sinopec, Beijing 100083, People's Republic of China. Email:wangyr.ripp@sinopec.com; luoyibin.ripp@sinopec.com

Contents

1. Detailed experimental procedures

1.1 Catalysts characterization

Phase identity and purity of the solid products were checked by powder XRD patterns using a PANalytical diffractometer with Cu KR radiation.

Elemental analysis for Siand Al was carried out by a Type 3013 X-Ray Fluorescence （XRF）Spectrometer from Nihon Riken Electric Co., Ltd.

The N_2 sorption experiments were performed on a Micromeritics ASAP 2010 Static Nitrogen Adsorption Instrument. The measurement method is as following, the sample was placed in the processing system, the vacuum was drawn to 1.33×10^{-2} Pa at 350 °C, and maintained for 15 h to purify the sample. At the liquid nitrogen temperature of -196 °C, the adsorption and desorption amounts of nitrogen were measured under different P/P_0 conditions, the adsorption-desorption isotherm curves were obtained. Then, the two-parameter BET formula was used to calculate the specific surface area, the adsorption volume below the specific pressure $P/P_0\approx0.98$ was taken as the pore volume of the sample.

Thermogravimetric (TG) analysis was conducted using a Netzsch STA 409CD simultaneous thermal analyzer (NETZSCH-Gerätebau GmbH, Bavaria, Germany). Approximately 5-10 mg of sample was placed in an alumina crucible and heated from 30 to 1200 °C at a heating rate of 10 °C/min. The experiments were performed under either air or argon atmosphere with a gas flow rate of 100 mL/min. The mass change and derivative thermogravimetric (DTG) curves were recorded continuously throughout the heating process to evaluate the thermal stability and decomposition behavior of the samples.

NH_3-TPD was measured with Micromeritics Autochem II 2920. Approximately 0.20-0.25 g of 20-40 mesh sample was loaded into a quartz tube and placed in a thermal conductivity detector (TCD) furnace. The sample was pretreated under He flow (20 mL/min) by heating to 600 °C (20 °C/min) for 60 min to remove adsorbed impurities. After cooling to 100 °C (held for 10 min), the gas was switched to an

NH_3/He mixture (10.02% NH_3, 89.98% He) for 30 min adsorption. Physically adsorbed NH_3 was removed by He purging (90 min) until baseline stabilization. The temperature was then ramped to 600 °C (10 °C/min, held for 30 min) to desorb chemisorbed NH_3. The TCD signal was recorded to generate the NH_3 adsorption–desorption profile, and the total acid amount was determined by automatic integration of the desorption peak.

Py-IR was collected by IR spectrometer(BIO-RAD FTS3000) using pyridine as probe molecule in the wavenumber range 1700-1300 cm^{-1}. The samples were pressed into lamina and activated at 400 ℃ for 1 h in vacuum(pressure $<10^{-5}$ Pa).After cooling to room temperature, a spectrum was recorded. Pyridine was then adsorbed at room temperature for 0.5h. The strength of the acid sites was probed by increasing the temperature to 200 ℃ and 350 ℃.

The gas chromatography-mass spectrometry (GC-MS) analysis was performed using an Agilent 7890B GC system coupled with an Agilent 5977A MSD mass spectrometer. The system was equipped with an HP-5MS capillary column (30 m × 0.25 mm × 0.25 μm). The oven temperature program was set as follows: initial temperature of 50 °C (hold for 2 min), ramped at 10 °C/min to 300 °C, and finally held for 3 min . The mass spectrometer was operated in electron ionization (EI) mode at 70 eV, with the ion source and quadrupole temperatures set at 230 °C and 150 °C, respectively. The mass range was scanned from m/z 35 to 350 at a rate of 4.5 scans per second. The solvent delay time was set to 3 min. Sample injection volume was 1 μL.

1.2 Substrate expansion

The reaction process is the same as that for the CDOX from CDON and CHO. Under the above similar reaction conditions (the reaction temperature, the ratio of raw materials of individual substrates increased or decreased, and the reaction time prolonged or shortened), the autoclave was cooled to room temperature after the reaction was completed, the reactants were washed out with solvent, and then the products were analyzed and characterized by GC.

1.3 Catalyst recycling test

After each reaction, the reaction mixture was cooled to room temperature and dissolved in anhydrous ethanol for analysis. The resulting solution was subjected to centrifugation to achieve solid-liquid separation and remove the solid catalyst residues. The catalyst was washed three times with 6 ml ethyl acetate each time, wash once with ethanol, and dried. It was then used directly in the next experiment to evaluate its stability.

1.4 Computational theory and methods

The molecular structures of the reactants and products were modeled and their molecular dimensions were calculated using Materials Studio 2020. The free energy of the reaction system was computed using density functional theory (DFT) with Gaussian 16, and the corresponding thermodynamic parameters were extracted using the Shermo program. Detailed computational procedures, including geometry optimization, single-point energy calculations, derivation of thermodynamic parameters, and the models and parameters used for molecular dimension calculations, are provided in Table S1 and Fig. 4(a).

2. Optimization of process conditions

2.1 Single-factor optimization data

Table S1. Thermodynamic parameters of the transoximation reaction

All quantum chemical calculations were performed using Gaussian 16. The molecular geometries of reactants (CHO, CDON) and products (CDOX, CYC) were first optimized at the B3LYP/6-31G(d) level of theory. To obtain more accurate electronic energies, single-point energy calculations were then conducted on the optimized geometries using the B3LYP functional with a combined basis set of 6-31G(d) and cc-pVDZ[1]. Finally, the standard enthalpy (H_T) and Gibbs free energy (G_T) for each species across the relevant temperature range (70-160 °C) were derived from the vibrational frequencies and refined single-point energies using the Shermo program[2]. The reaction enthalpy change ($\triangle_r H_T$) and Gibbs free energy change ($\triangle_r G_T$) were obtained from:

$\Delta_r X = \sum X_{products} - \sum X_{reactants}$, where X represents H_T or G_T.

Finally, the equilibrium constant K_T at each temperature was determined from: $\Delta_r G_T = -RTlnK_T$, where R=8.314 J·mol^{-1}·K^{-1} ,T is the absolute temperature.

T/ °C	T/K	$\triangle_r H_T$/KJ·mol^{-1}	$\triangle_r G_T$/KJ·mol^{-1}	K_T
70	343.15	17.00	8.96	0.043
80	353.15	17.65	8.24	0.060
90	363.15	18.30	7.51	0.083
100	373.15	18.97	6.77	0.113
110	383.15	19.64	6.01	0.152
120	393.15	20.32	5.23	0.202
130	403.15	21.01	4.44	0.266
140	413.15	21.70	3.63	0.347
150	423.15	22.40	2.81	0.450
160	433.15	23.11	1.98	0.577

Table S2. Effect of reaction temperature on the transoximation reaction

Temperature/°C	Reaction/%				Reaction-Distillation			
	Conv.$_{xx,R}$ /%		Sel.$_{xx,R}$/%		Conv.$_{xx,R}$ /%		Sel.$_{xx,R}$/%	
	CHO	CDON	CDOX	LAU	CHO	CDON	CDOX	LAU
70	32.12	26.78	100	0	80.78	67.32	100	0
80	36.46	32.88	100	0	84.24	69.37	100	0
90	39.87	33.15	100	0	86.87	72.39	100	0
100	45.07	37.56	95.88	4.12	88.84	74.03	94.32	5.68
120	52.34	43.62	87.67	12.33	91.13	75.94	85.37	14.63
160	58.33	48.61	64.53	35.47	93.32	77.77	61.58	38.42

a-Reaction conditions: Zeolite (1.4 g), CDON(2.21 g):CHO(1.16 g) = 1.2:1 (molar ratio), 9 h

b-Reaction conditions: Zeolite (1.4 g), CDON(2.21 g):CHO(1.16 g) = 1.2:1 (molar ratio), 9 h, vacuum degree(240 mbar)

Table S3. Effect of vacuum degree on the transoximation reaction

Vacuum degree/mbar	R_{CYC}/%	Conv.$_{CHO,RD}$/%	Conv.$_{CDON,RD}$/%	Sel.$_{CDOX,RD}$ /%
0	0.00	42.37	35.31	100
120	6.66	47.22	39.35	100
160	21.77	56.35	46.96	100
200	75.11	78.22	65.18	100
240	99.98	92.22	76.85	100
280	99.98	82.42	68.68	100

Reaction conditions: HY zeolite (1.4 g), CDON(2.21 g):CHO(1.16 g) = 1.2:1 (molar ratio), 9 h, vacuum degree(0-280 mbar), temperature(90 °C)

Table S4. Effect of catalyst amount on the transoximation reaction

Catalyst(g)	Conv.$_{\mathrm{CHO,RD}}$/%	Conv.$_{\mathrm{CDON,RD}}$/%	Sel.$_{\mathrm{CDOX,RD}}$ /%	Sel.$_{\mathrm{LAU,RD}}$ /%	R$_{\mathrm{CYC}}$/%
0.6	58.32	48.61	100.00	0.00	0.05
1.0	72.34	60.28	100.00	0.00	0.03
1.2	86.68	72.23	100.00	0.00	0.02
1.4	92.22	76.85	100.00	0.00	0.03
1.6	94.38	78.65	100.00	0.00	0.02
1.8	98.34	81.95	98.70	1.30	0.04

Reaction conditions: HY zeolite (0.6-1.8 g), CDON(2.21 g):CHO(1.16 g) = 1.2:1 (molar ratio), 9 h, vacuum degree(240 mbar), temperature(90 °C)

Table S5. Effect of CDON/CHO molar ratio on the transoximation reaction

Molar Ratio	Conv.$_{\mathrm{CHO,RD}}$/%	Conv.$_{\mathrm{CDON,RD}}$/%	Sel.$_{\mathrm{CDOX,RD}}$ /%	Sel.$_{\mathrm{LAU,RD}}$ /%	R$_{\mathrm{CYC}}$/%
1:1	85.32	85.32	100.00	0.00	0.02
1.2:1	94.38	78.65	100.00	0.00	0.03
1.4:1	98.08	70.06	100.00	0.00	0.02
1.6:1	98.87	61.79	100.00	0.00	0.03
1.8:1	99.04	55.02	100.00	0.00	0.01

Reaction conditions: HY zeolite (1.6 g), CDON:CHO(1.16 g) = 1-1.8:1 (molar ratio), 9 h, vacuum degree(240 mbar), temperature(90 °C)

Table S6. Effect of reaction time on the transoximation reaction

Time/h	Conv.$_{CHO,RD}$/%	Conv.$_{CDON,RD}$/%	Sel.$_{CDOX,RD}$ /%	Sel.$_{LAU,RD}$ /%	R$_{CYC}$/%
6	92.32	65.94	100.00	0.00	0.01
7	95.81	68.43	100.00	0.00	0.02
8	97.21	69.44	100.00	0.00	0.02
9	98.08	70.06	100.00	0.00	0.02
10	99.45	71.03	100.00	0.00	0.02
11	99.54	71.10	100.00	0.00	0.01

Reaction conditions: HY zeolite (1.6 g), CDON(2.58 g):CHO(1.16 g) = 1.4:1 (molar ratio), 6-11 h, vacuum degree(240 mbar), temperature(90 °C)

2.2 Plackett-Burman[3] design analysis

Based on the single-factor experimental findings, a P-B design was employed to systematically screen the factors influencing the solvent-free transoximation reaction. Five factors:temperature (A), vacuum degree (B), molar ratio(CDON:CHO) (C), catalyst dosage (D), and reaction time (E) were evaluated at two levels to identify the primary variables for subsequent response surface optimization. The complete experimental design matrix and results for both Conv.$_{CHO,RD}$ and Sel.$_{CDOX,RD}$ are presented in Table S7.

Table S7 P-B experimental design matrix and results

Run	A	B	C	D	E	Conv.$_{CHO,RD}$/%	Sel.$_{CDOX,RD}$ /%
1	+1	+1	-1	+1	+1	80.21	87.52
2	-1	+1	+1	-1	+1	84.12	100.00
3	+1	-1	+1	+1	-1	96.28	89.22
4	-1	+1	-1	+1	+1	78.48	100.00
5	-1	-1	+1	-1	+1	77.45	100.00
6	-1	-1	-1	+1	-1	68.93	100.00
7	+1	-1	-1	-1	+1	76.22	92.17
8	+1	+1	-1	-1	-1	67.58	92.96
9	+1	+1	+1	-1	-1	83.84	90.51
10	-1	+1	+1	+1	-1	88.42	100.00
11	+1	-1	+1	+1	+1	98.72	88.17
12	-1	-1	-1	-1	-1	57.33	100.00

Table S8. Analysis of variance for Conv.$_{\mathrm{CHO,RD}}$

Source	Sum of Squares	Mean Square	F-Value[b]	p-Value	Significance
Model[a]	1469.05	293.81	28.23	0.0004	***
Temperature/°C	192.96	192.96	18.54	0.0051	**
Vacuum degree/mbar	4.97	4.97	0.48	0.5155	ns
Molar ratio(CDON:CHO)	834.67	834.67	80.21	0.0001	***
Catalyst dosage/g	346.69	346.69	33.33	0.0012	***
Reaction time/h	89.76	89.76	8.63	0.0260	*
Residual	62.43	10.41	-	-	-
Total	1531.48	-	-	-	-

***$p < 0.001$(most significant); **$p < 0.01$(highly significant); *$p < 0.05$(significant); ns: not significant

a-Multiple linear regression analysis was performed using Design-Expert software to establish preliminary relationships between the Conv.$_{\mathrm{CHO,RD}}$ and the five independent variables. The empirical linear models correlating the responses with reaction temperature (A), vacuum degree (B), molar ratio(CDON:CHO) (C), catalyst dosage (D), and reaction time (E) were expressed as first-order polynomial equations:

Conv.$_{\mathrm{CHO,RD}}$ /%:

$$Y_1 = 79.80 + 4.01A + 0.6433B + 8.34C + 5.38D + 2.73E$$

Y_1: Predicted Conv. $_{\mathrm{CHO,RD}}$ based on the linear model from the P-B design

Model Statistics: Coefficient of Determination (R^2) = 0.9592, Adjusted Coefficient of Determination(Adjusted R^2) = 0.9253, Coefficient of Variatio (CV) = 0.4040 ($\mathrm{CV} = \frac{\sqrt{\text{Mean Square of the Residual}}}{\text{Mean}}$), Mean = 79.80% (The average value of the Conv.$_{\mathrm{CHO,RD}}$ across all experimental runs.)

b-The F-value is a test statistic in Analysis of Variance (ANOVA). It is calculated as the ratio of the mean square of a source to the mean square of a residual. $F\text{-}Value = \frac{Mean\,Square\,of\,the\,source}{Mean\,Square\,of\,the\,residual} \times 100\%$. A larger F-value indicates that the variation caused by the source is much greater than the variation caused by residual. Therefore, that factor or model is considered more statistically significant.

The ANOVA results for Conv.$_{\mathrm{CHO,RD}}$ were presented in Table S8. The F-value and P-value ($F = 28.23$, $p = 0.0006$) of the model indicated that the selected factors have a significant impact on the Conv.$_{\mathrm{CHO,RD}}$. The R^2 (0.9592) and adjusted R^2 (0.9253) indicated excellent model fit. The relatively low CV=0.4040) confirmed good experimental precision and reproducibility.

Table S9. Main Effects of factors on Conv.$_{CHO,RD}$

Factor	Effect/%[a]	Low Level/%	High Level/%	F-Value	p-Value	Rank
Molar ratio(CDON:CHO)	+16.68	71.46	88.14	80.21	0.0001	1
Catalyst dosage/g	+10.75	74.42	85.17	33.33	0.0012	2
Temperature/°C	+8.02	75.79	83.81	18.54	0.0051	3
Reaction time/h	+5.47	77.06	82.53	8.63	0.0260	4
Vacuum degree/mbar	+1.29	79.16	80.44	0.48	0.5155	5

a-The Effect of a factor in a designed experiment means that the average change in the Conv.$_{CHO,RD}$ when one of the factors is changed from a low level to a high level, while keeping all other factors constant. The average change value shows the direction and magnitude of the influence of this factor on the Conv.$_{CHO,RD}$

$$Effect = High\ Level - Low\ Level$$

Positive Effect (+): Increasing the factor level increases the Conv.$_{CHO,RD}$.

Negative Effect (-): Increasing the factor level decreases the Conv.$_{CHO,RD}$.

Magnitude: The absolute value indicates the strength of the influence.

Table S10. Analysis of variance for $\text{Sel.}_{\text{CDOX,RD}}$

Source	Sum of Squares	Mean Square	F-Value	p-Value	Significance
Model[a]	308.11	61.62	36.25	0.0002	***
Temperature/° C	294.52	294.52	173.27	0.0001	***
Vacuum degree/mbar	0.17	0.17	0.10	0.7623	ns
Molar ratio(CDON:CHO)	1.88	1.88	1.11	0.3334	ns
Catalyst dosage/g	9.59	9.59	5.64	0.0551	ns
Reaction time/h	1.94	1.94	1.14	0.3260	ns
Residual	10.20	1.70	-	-	-
Total	318.31	-	-	-	-

***$p < 0.001$(most significant); ns: not significant

a-Multiple linear regression analysis was performed using Design-Expert software to establish preliminary relationships between the $\text{Sel.}_{\text{CDOX,RD}}$ and the five independent variables. The empirical linear models correlating the $\text{Sel.}_{\text{CDOX,RD}}$ with reaction temperature (A), vacuum degree (B), molar ratio(CDON: CHO) (C), catalyst dosage (D), and reaction time (E) were expressed as first-order polynomial equations:

$\text{Sel.}_{\text{CDOX,RD}}$ /%:

$$Y_2 = 95.05 - 4.95A + 0.1192B - 0.3958C - 0.8942D - 0.4025E$$

Y_2: Predicted $\text{Sel.}_{\text{CDOX,RD}}$ based on the linear model from the P-B design

Model Statistics: R^2 =0.9680, Adjusted R^2=0.9413, CV=0.1370, Mean=95.05% (The average value of the $\text{Sel.}_{\text{CHO,RD}}$ across all experimental runs.)

The ANOVA results for $\text{Sel.}_{\text{CHO,RD}}$ were presented in Table S10. The F-value and P-value (F = 36.25, p = 0.0002) of the model indicated that the selected factors have a significant impact on the $\text{Sel.}_{\text{CHO,RD}}$. The R^2 (0.9680) and adjusted R^2 (0.9413) indicated excellent model fit. The relatively low (CV = 0.1370) confirmed good experimental precision and reproducibility.

Table S11. Main effects of factors on Sel.$_{\mathrm{CDOX,RD}}$

Factor	Effect /%	Low Level /%	High Level /%	F-Value	p-Value	Rank
Temperature/°C	-9.91	100.00	90.09	173.27	0.0001	1
Catalyst dosage/g	-1.79	95.94	94.15	5.64	0.0551	2
Reaction time/h	-0.81	95.45	94.64	1.14	0.3260	3
Molar ratio(CDON:CHO)	-0.79	95.44	94.65	1.11	0.3334	4
Vacuum degree/mbar	+0.24	94.93	95.17	0.10	0.7632	5

a-The Effect of a factor in a designed experiment means that the average change in the Sel.$_{\mathrm{CHO,RD}}$ when one of the factors is changed from a low level to a high level, while keeping all other factors constant. The average change value shows the direction and magnitude of the influence of this factor on the Sel.$_{\mathrm{CHO,RD}}$

$$Effect = High\ Level - Low\ Level$$

Positive Effect (+): Increasing the factor level increases the Sel.$_{\mathrm{CHO,RD}}$.

Negative Effect (-): Increasing the factor level decreases the Sel.$_{\mathrm{CHO,RD}}$.

Magnitude: The absolute value indicates the strength of the influence.

2.3 Box-Behnken[4] design analysis

The Box-Behnken experimental design matrix comprising 17 runs and the corresponding experimental responses are presented in Table S12. The results showed that $\mathrm{Conv.}_{\mathrm{CHO,RD}}$ ranged from 84.35% to 99.64%, while $\mathrm{Sel.}_{\mathrm{CDOX,RD}}$ varied between 93.25% and 100.00% across different experimental conditions. The maximum $\mathrm{Conv.}_{\mathrm{CHO,RD}}$ (99.64%) was achieved at run 16, which corresponded to the center point conditions. Notably, runs conducted at lower temperature levels (runs 1, 3, 5, 7, 9, 11, and 12) consistently exhibited 100.00% $\mathrm{Sel.}_{\mathrm{CDOX,RD}}$, suggesting that temperature plays a critical role in determining product selectivity.

The five replicated center point experiments (runs 13-17) were performed to evaluate the reproducibility and experimental error. The $\mathrm{Conv.}_{\mathrm{CHO,RD}}$ obtained were 99.45%, 99.23%, 98.87%, 99.64%, and 98.38%, respectively, with a mean value of 99.11%, standard deviation of 0.46%, and relative standard deviation of 0.46%. This excellent reproducibility confirmed the high precision and reliability of the experimental methodology, indicating that the experimental procedures were well-controlled and the analytical methods were accurate.

Table S12. Box-Behnken[4] experimental design matrix and responses

Run	A	B	C	Conv.$_{CHO,RD}$/%	Sel.$_{CDOX,RD}$ /%
1	-1	-1	0	84.35	100.00
2	+1	-1	0	94.78	93.87
3	-1	+1	0	89.76	100.00
4	+1	+1	0	99.57	93.25
5	-1	0	-1	87.32	100.00
6	+1	0	-1	97.85	94.13
7	-1	0	+1	90.87	100.00
8	+1	0	+1	98.78	93.56
9	0	-1	-1	89.56	100.00
10	0	+1	-1	98.78	100.00
11	0	-1	+1	92.59	100.00
12	0	+1	+1	99.34	100.00
13	0	0	0	99.45	100.00
14	0	0	0	99.23	100.00
15	0	0	0	98.87	100.00
16	0	0	0	99.64	100.00
17	0	0	0	98.38	100.00

Table S13. ANOVA results for Conv.$_{\mathrm{CHO,RD}}$ response surface quadratic model

Source	Sum of Squares	Mean Square	F-Value[b]	p-Value	Significance
Model[a]	407.75	45.31	55.96	< 0.0001	***
A-Temperature/°C	187.02	187.02	231.01	< 0.0001	***
B-Molar ratio(CDON:CHO)	85.61	85.61	105.75	< 0.0001	***
C-Catalyst dosage/g	8.14	8.14	10.06	0.0157	*
AB	0.0961	0.10	0.12	0.7406	ns
AC	1.72	1.72	2.12	0.1887	ns
BC	1.53	1.53	1.88	0.2122	ns
A^2	73.59	73.59	90.91	< 0.0001	***
B^2	33.44	33.44	41.31	0.0004	***
C^2	6.35	6.35	7.85	0.0265	*
Residual	5.67	0.81	-	-	-
Lack of Fit	4.67	1.56	6.21	0.0550	-
Pure Error	1.00	0.25	-	-	-
Cor Total	413.42	-	-	-	-

*** $p < 0.001$ (most significant); * $p < 0.05$ (significant); ns: not significant

a-Multiple regression analysis was performed using Design-Expert software to establish mathematical relationships between the responses and the three independent variables. The empirical models correlating Conv.$_{\mathrm{CHO,RD}}$ with reaction temperature (A), molar ratio(CDON:CHO) (B), and catalyst dosage (C) were expressed as second-order polynomial equations:

Conv.$_{\mathrm{CHO,RD}}$ /%:

$$Y_3 = 99.11 + 4.82A + 3.27B + 1.01C - 0.155AB - 0.655AC - 0.6175BC - 4.18A^2 - 2.82B^2 - 1.23C^2$$

Y_3: Predicted Conv. $_{CHO,RD}$ based on the quadratic model from the Box-Behnken design.

b-The F-value is a test statistic in Analysis of Variance (ANOVA). It is calculated as the ratio of the mean square of the source to the mean square of the residual. It quantifies whether the variance explained by the source is significantly greater than the unexplained random variance in the data. $F\text{-}Value = \frac{Mean\ Square\ of\ the\ Source}{Mean\ Square\ of\ the\ Residual} \times 100\%$,

The ANOVA results for the Conv.$_{CHO,RD}$ model revealed a high F-value (55.96) with a very low p-value (< 0.0001), indicating that the model was the most significant. These statistical parameters confirmed the reliability of the Conv.$_{CHO,RD}$ model.

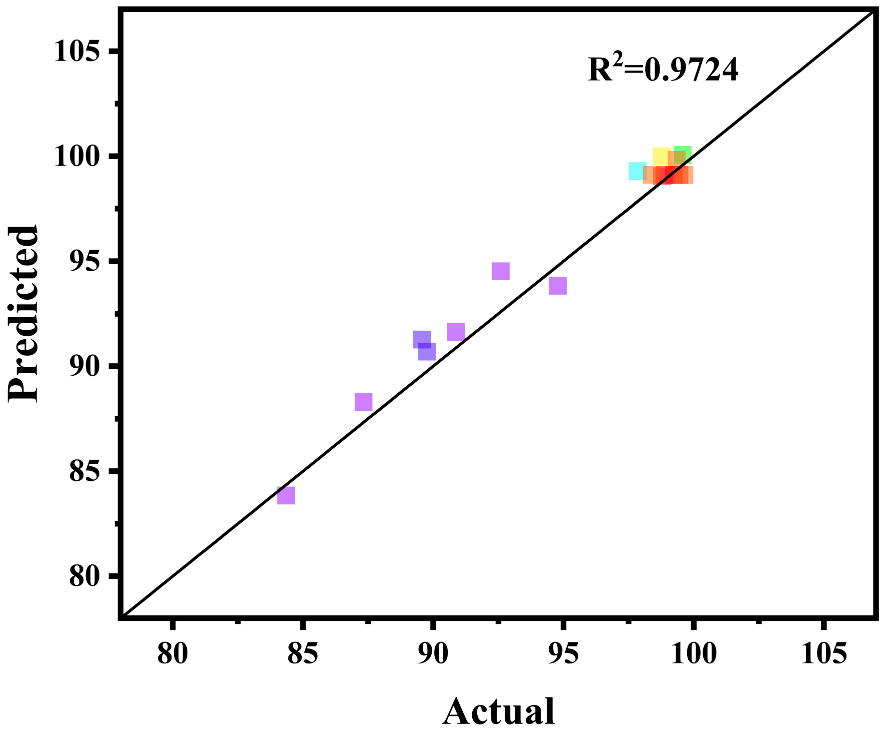

Fig. S1. Scatter plot of predicted and actual values of Conv.$_{CHO,RD}$ designed by RSM

Fig. S1 shows the results of the actual (experimental) values of Conv.$_{CHO,RD}$ against the predicted values 0.9724, which indicates reasonable precision between the data and the model.

Table S14. ANOVA results for $\text{Sel.}_{\text{CDOX,RD}}$ response surface quadratic model

Source	Sum of Squares	Mean Square	F-Value	p-Value	Significance
Model[a]	121.61	13.51	731.69	< 0.0001	***
A-Temperature/°C	79.32	79.32	4294.87	< 0.0001	***
B-Molar ratio(CDON:CHO)	0.0481	0.0481	2.60	0.1508	ns
C-Catalyst dosage/g	0.0406	0.0406	2.20	0.1817	ns
AB	0.0961	0.0961	5.20	0.0565	ns
AC	0.0812	0.0812	4.40	0.0742	ns
BC	0.0000	0.0000	0.0000	1.0000	ns
A^2	41.75	41.75	2260.46	< 0.0001	***
B^2	0.0214	0.0214	1.16	0.3177	ns
C^2	0.0214	0.0214	1.16	0.3177	ns
Residual	0.1293	0.0185	-	-	-
Lack of Fit	0.1293	0.0431	-	-	-
Pure Error	0.0000	0.0000	-	-	-
Cor Total	121.74	-	-	-	-

***$p < 0.001$(most significant); **$p < 0.01$(highly significant); *$p < 0.05$(significant); ns: not significant

a-Multiple regression analysis was performed using Design-Expert software to establish mathematical relationships between the responses and the three independent variables. The empirical models correlating $\text{Sel.}_{\text{CDOX,RD}}$ with reaction temperature (A), molar ratio(CDON: CHO) (B), and catalyst dosage (C) were expressed as second-order polynomial equations:

$\text{Sel.}_{\text{CDOX,RD}}$ /%:

$$Y_4 = 100 - 3.15A - 0.0775B - 0.0712C - 0.155AB - 0.1425AC +$$

$$0BC - 3.15A^2 - 0.0712B^2 + 0.0712C^2$$

Y_4: Predicted $\text{Sel.}_{\text{CDOX,RD}}$ based on the quadratic model from the Box-Behnken design.

The ANOVA results for the $\text{Sel.}_{\text{CDOX,RD}}$ model showed an even higher F-value (731.69) with a very low p-value (< 0.0001), indicating that the model was the most significant. The superior statistical performance of this model confirmed its high reliability for $\text{Sel.}_{\text{CDOX,RD}}$.

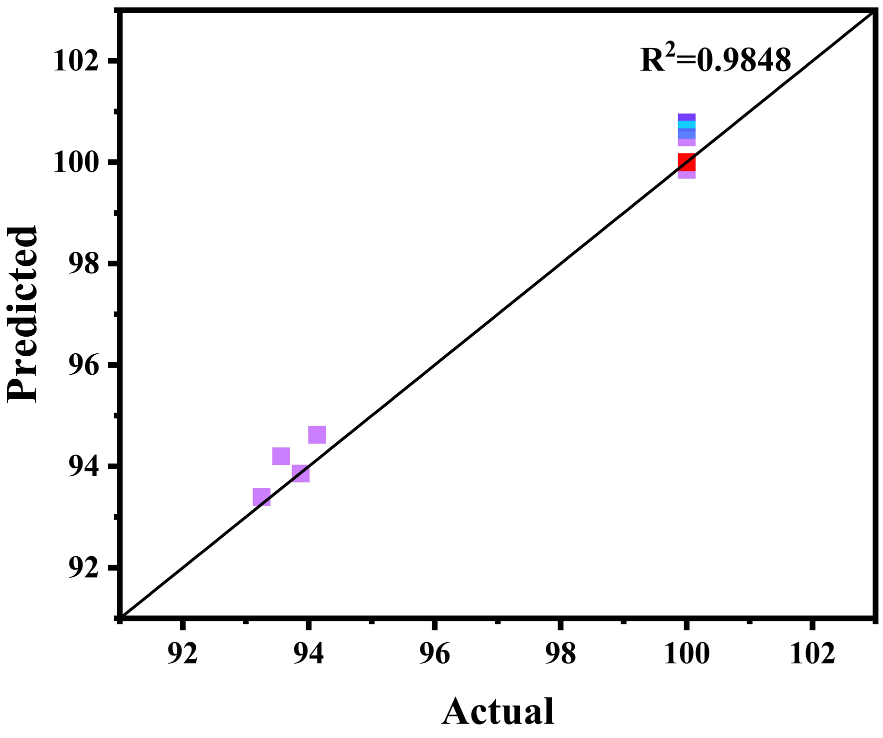

Fig. S2. Scatter plot of predicted and actual values of Sel. $_{\mathrm{CDOX,\ RD}}$ designed by RSM

Fig. S2 shows the results of the actual (experimental) values of Sel. $_{\mathrm{CDOX,\ RD}}$ against the predicted values of the response surface method. The value of the determination coefficient (R^2) is 0.9848, which indicates reasonable precision between the data and the model.

3. The physico-chemical properties of zeolite

Table S15. Acidity properties of the zeolite catalysts.

Zeolites	$n(SiO_2)/n(Al_2O_3)$	Acid density/μmol·g^{-1a}	Acid amount /μmol^{b}
HY	5	1532.3	2451.7
HBeta	21	1412.5	2260.0
HMOR	20	1355.8	2169.3
HZSM-5	27	1338.4	2141.4

a-The density of acid was measured using the NH_3-TPD approach.

b-The quantity of acid equals the acid density multiplied by the catalyst’s mass.

Table S16. Structural parameters of selected zeolites.

Zeolites	Framework Type Code	Channel Ring Size	Pore Size /Å	Freely Diffusing Diameter[a] /Å	Included Molecule Diameter[b]/Å
HY	FAU	12	7.4×7.4	7.35	11.24
HBeta	BEA	12	6.6×6.9 5.6×5.6	6.09	6.95
HMOR	MOR	12	6.5×7.0 2.6×5.7	6.45	6.71
HZSM-5	MFI	10	5.1×5.5 5.3×5.6	4.46	6.36

a- Freely diffusing diameter: The maximum diameter of a spherical molecule that can diffuse freely along the channel system.

b- Included molecule diameter: The maximum diameter of a spherical molecule that can be accommodated within the largest cavity.

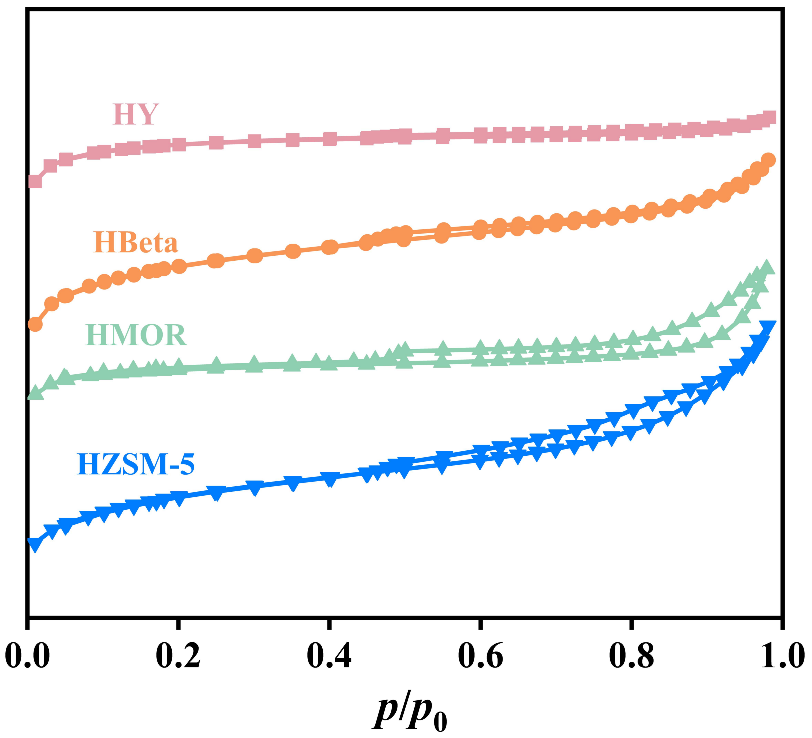

Fig. S3. BET patterns of the four zeolite samples (HY, HBeta, HMOR, and HZSM-5).

Table S17. Surface area and pore volume characteristics of different zeolites

Zeolites	S_{BET}/$m^2 \cdot g^{-1}$	S_{micro}/$m^2 \cdot g^{-1}$	$S_{external}$/$m^2 \cdot g^{-1}$	V_{pore}/$cm^3 \cdot g^{-1}$	V_{micro}/$cm^3 \cdot g^{-1}$	V_{meso}/$cm^3 \cdot g^{-1}$
HY	678.905	670.167	8.739	0.326	0.309	0.017
HBeta	591.296	477.056	114.239	0.428	0.221	0.207
HMOR	341.836	329.680	12.155	0.208	0.152	0.056
HZSM-5	349.331	330.512	18.819	0.181	0.152	0.029

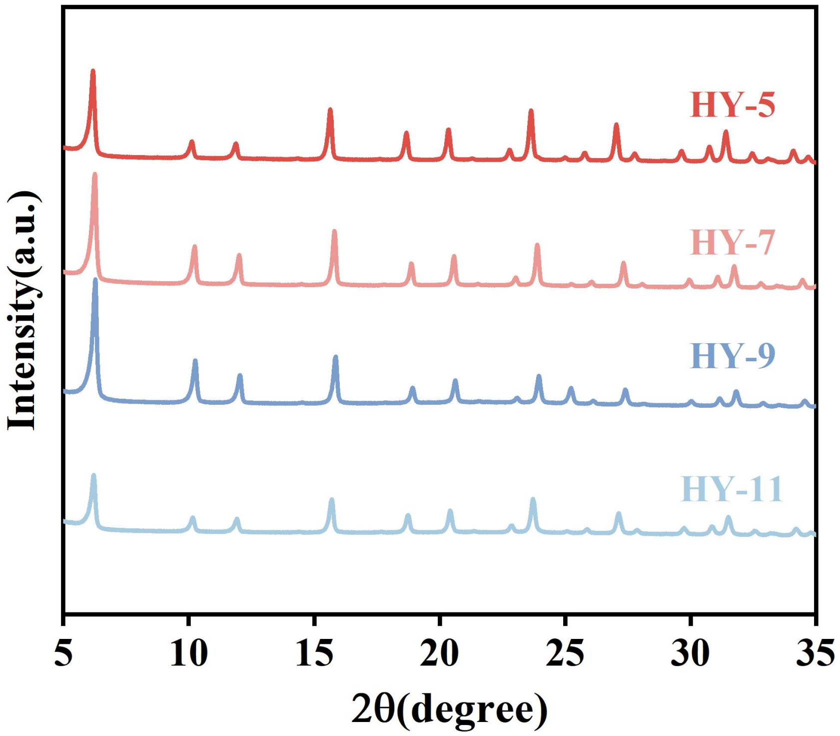

Fig. S4. XRD patterns of HY-R zeolites

Table. S18. Crystallinity and n(SiO_2)/n(Al_2O_3) of HY-R zeolites

Zeolite	Crystallinity/%	n(SiO_2)/n(Al_2O_3)
HY-5	76.8	4.92
HY-7	78.2	6.97
HY-9	75.7	9.21
HY-12	74.3	11.72

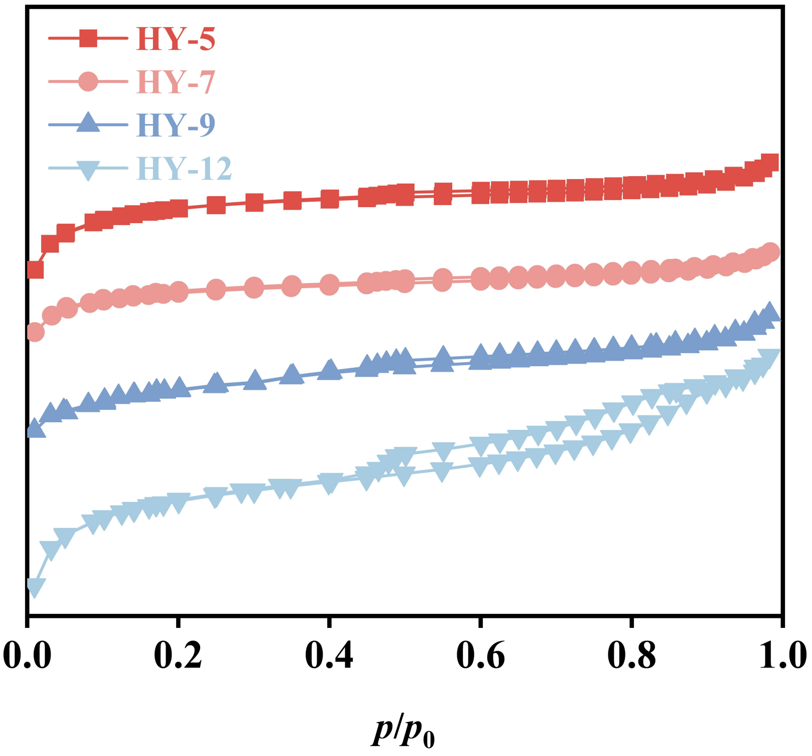

Fig. S5. N_2 adsorption/desorption curves of HY-R zeolites

Table. S19. Specific surface area and pore volume of HY-R zeolites

Zeolites	S_{BET}/$m^2 \cdot g^{-1}$	S_{micro}/$m^2 \cdot g^{-1}$	$S_{external}$/$m^2 \cdot g^{-1}$	V_{pore}/$cm^3 \cdot g^{-1}$	V_{micro}/$cm^3 \cdot g^{-1}$	V_{meso}/$cm^3 \cdot g^{-1}$
HY-5	678.905	670.167	8.739	0.326	0.309	0.017
HY-7	642.912	618.216	24.695	0.309	0.285	0.024
HY-9	618.678	604.857	13.821	0.280	0.246	0.034
HY-12	574.224	557.797	16.427	0.243	0.194	0.050

4. Reaction mechanism speculation

Table S20. Static water adsorption performance of HY-5 under different NaCl solution conditions

Zeolites	NaCl Solution Concentration /wt%	Mass^a /g	Mass^b /g	Static Water Adsorption Capacity /%^{a}
HY-5	-	2.00	2.00	0.00
HY-5-30	26 .00(saturated)	2.00	2.61	30.50
HY-5-37	13.00	2.00	2.75	37.50
HY-5-44	0.00	2.00	2.89	44.50

a-Mass: mass of zeolite after calcination

b-Mass:mass of zeolite after 24 h adsotption

c-Static water adsorption capacity is calculated as: (Mass^a - Mass^b) / Mass^a ×100%

Table S21. Catalytic performance of HY-5-X zeolites with distillation

Zeolites	$\mathrm{Conv.}_{\mathrm{CHO,RD}}$/%	$\mathrm{Conv.}_{\mathrm{CDON,RD}}$/%	$\mathrm{Sel.}_{\mathrm{CDOX,RD}}$ /%	$\mathrm{Sel.}_{\mathrm{LAU,RD}}$ /%[a]	$\Delta\mathrm{Conv.}_{\mathrm{CHO,RD,X}}$/%[a]
HY-5	99.45	71.04	100.00	0.00	0.00
HY-5-30	99.73	71.23	100.00	0.00	0.28
HY-5-37	99.77	71.26	100.00	0.00	0.32
HY-5-44	99.81	71.29	100.00	0.00	0.36

Reaction conditions: Zeolite (1.6 g), CDON(2.58 g):CHO(1.16 g) = 1.4:1 (molar ratio), 10 h, vacuum degree(240 mbar), temperature(90 °C)

References

1 T.-T. Wang, Y. Shi, S. Li, Z.-H. Luo and Y.-N. Zhou, *Macromolecules*, 2023, **56**, 7379–7388.

2 T. Lu and Q. Chen, *Comput. Theor. Chem*., 2021, **1200**, 113249.

3 A. P. Karlapudi, S. Krupanidhi, R. R. E, I. M, N. B. Md and T. C. Venkateswarulu, Beni-Suef Univ. J. *Basic Appl. Sci.*, 2018, **7**, 543-546.

4 M. Mourabet, A. El Rhilassi, H. El Boujaady, M. Bennani-Ziatni and A. Taitai, *Arabian J. Chem.*, 2017, **10**, S3292-S3302.